

See discussions, stats, and author profiles for this publication at: <https://www.researchgate.net/publication/231645131>

Facile Synthesis of Mesoporous TiO₂-C Nanosphere as an Improved Anode Material for Superior High Rate 1.5 V Rechargeable Li Ion Batteries Containing LiFePO₄-C Cathode

ARTICLE *in* THE JOURNAL OF PHYSICAL CHEMISTRY C · MAY 2010

Impact Factor: 4.77 · DOI: 10.1021/jp103218u

CITATIONS

73

READS

24

5 AUTHORS, INCLUDING:



Xing-Long Wu

Northeast Normal University

61 PUBLICATIONS 3,008 CITATIONS

[SEE PROFILE](#)



Sen Xin

Hefei University of Technology

43 PUBLICATIONS 1,684 CITATIONS

[SEE PROFILE](#)



Yu-Guo Guo

Chinese Academy of Sciences

168 PUBLICATIONS 10,204 CITATIONS

[SEE PROFILE](#)

Facile Synthesis of Mesoporous $\text{TiO}_2\text{--C}$ Nanosphere as an Improved Anode Material for Superior High Rate 1.5 V Rechargeable Li Ion Batteries Containing $\text{LiFePO}_4\text{--C}$ Cathode

Fei-Fei Cao,[†] Xing-Long Wu,[†] Sen Xin,[†] Yu-Guo Guo,* and Li-Jun Wan*

Beijing National Laboratory for Molecular Sciences, Institute of Chemistry, Chinese Academy of Sciences (CAS), Beijing 100190, People's Republic of China

Received: April 10, 2010; Revised Manuscript Received: May 2, 2010

Well-organized mesoporous $\text{TiO}_2\text{--C}$ nanospheres are manufactured in large scale starting from tetrabutyl titanate (TBT) and glucose in solution, and investigated with scanning electron microscopy, transmission electron microscopy, X-ray diffraction, N_2 adsorption–desorption isotherms, and electrochemical experiments. The $\text{TiO}_2\text{--C}$ nanospheres show excellent rate capability and cycling performance for lithium ion batteries. At the extremely high rate of 100 C (discharge/charge within 36 s), the $\text{TiO}_2\text{--C}$ nanosphere can still deliver a specific capacity as high as 96 mA h g^{-1} . Moreover, the as-obtained mesoporous $\text{TiO}_2\text{--C}$ nanosphere can be used as an anode material for a new high rate 1.5 V rechargeable Li ion full cell containing a $\text{LiFePO}_4\text{--C}$ cathode with similar mixed conducting 3D networks. This type of rechargeable battery typically gives an output of 1.5 V per cell, which raises the potential for directly replacing the widely used 1.5 V primary alkaline batteries and dry cells.

1. Introduction

During the last century, traditional portable consumer electronics have been mainly powered by primary (nonrechargeable) alkaline batteries and dry cells with a nominal voltage of 1.5 V.^{1,2} After stepping into the 21st century, an increasing awareness of environmental protection and sustainable development has brought about the need for more cost-effective, environment- and user-friendly 1.5 V rechargeable batteries. Among all rechargeable battery systems, Ni–Cd batteries fail to meet the demand of green energy, while Ni–MH batteries and Li ion batteries though they possess environmental friendliness, are not able to deliver a nominal voltage suitable for portable electronics powered by primary batteries (e.g., 1.25 V for Ni–MH batteries and 3.7 V for commercial Li ion batteries).^{3–6} Though higher output voltage of batteries is favorable for powering future electric vehicles (EV) and plug-in electric vehicles (PEV), it is not good for powering portable electronics, because the voltage change is inconvenient for consumers. Therefore, a new type of green and rechargeable battery with an output voltage of 1.5 V is highly desired.^{3,7–10} The success of this rechargeable battery may not only power the existing devices without any change in electrical circuits, but also may lead to a more powerful clean energy source with high power performance.

Among various cathode materials investigated for Li ion battery, LiFePO_4 appears to be a promising material to replace the current one with Co-based cathode materials which pose problems associated with cost and environmental hazard.¹¹ So far, high-rate $\text{LiFePO}_4\text{--C}$ cathode material has been successfully synthesized.^{11,12} As the insertion/extraction of lithium in LiFePO_4 occurs at a potential of approximately 3.4 V versus Li^+/Li ,^{11,12} an anode with the potential of about 1.9 V versus Li^+/Li is desired to assemble the 1.5 V full rechargeable Li ion cell.^{13–15}

Though $\text{Li}_4\text{Ti}_5\text{O}_{12}$, as a “zero-strain” insertion host material, has an extremely long cycle life, its flat Li insertion potential is located at about 1.55 V (versus Li^+/Li), which leads to the output voltage of a $\text{Li}_4\text{Ti}_5\text{O}_{12}/\text{LiFePO}_4$ cell being not 1.5 V but about 1.8 V. Indeed, anatase TiO_2 could be considered a good match because the potential of lithium insertion/extraction of it is about 0.3 V higher than that of $\text{Li}_4\text{Ti}_5\text{O}_{12}$ (~1.9 V versus Li^+/Li).¹⁶ However, TiO_2 has been reported to suffer from a key problem in application as an anode material because of its poor electronic conductivity.¹⁶ Various synthetic and processing approaches have been employed to solve this problem, which include exploiting three-dimensional (3D) network-like structures,^{8,17–19} conductive coatings,²⁰ introducing conductive additives, as well as using mesoporous structures.¹⁶ Superior rate performance has been reported for mesoporous nanostructured networks of $\text{TiO}_2\text{--RuO}_2$ and $\text{TiO}_2\text{--SWCNT}$ (single-walled carbon nanotube) composite for which good electronic wiring is a necessary condition.^{16,21} However, to become commercially viable, a cost-effective coating material such as carbon is desired to replace the expensive RuO_2 or SWCNT.

Here, we demonstrate an inexpensive and industrially scalable method to coat porous anatase TiO_2 nanospheres with electrically conductive carbon coating layers. Mesoporous $\text{TiO}_2\text{--C}$ nanospheres were manufactured in large scale starting from tetrabutyl titanate (TBT) and glucose in solution. First, mesoporous TiO_2 nanospheres are prepared by an ethylene glycol mediated process,²² after that, the carbon precursor layers were introduced into the porous TiO_2 spheres by pyrolysis of glucose under hydrothermal conditions. Finally, the $\text{TiO}_2\text{--C}$ composite precursor was calcined under Ar atmosphere to obtain good electrical conductivity. Then, as-obtained mesoporous $\text{TiO}_2\text{--C}$ nanosphere shows a superior high rate capability when used as the anode material for lithium half cells (against a Li counter electrode). Furthermore, new high rate 1.5 V rechargeable Li ion full cells are fabricated based on the $\text{TiO}_2\text{--C}$ anode and a $\text{LiFePO}_4\text{--C}$ cathode showing good rate performance.¹¹

* To whom correspondence should be addressed. E-mail: ygguo@iccas.ac.cn (Y.-G.G.) and wanlijun@iccas.ac.cn (L.-J.W.).

[†] Also at the Graduate School of CAS, Beijing 100064, People's Republic of China.

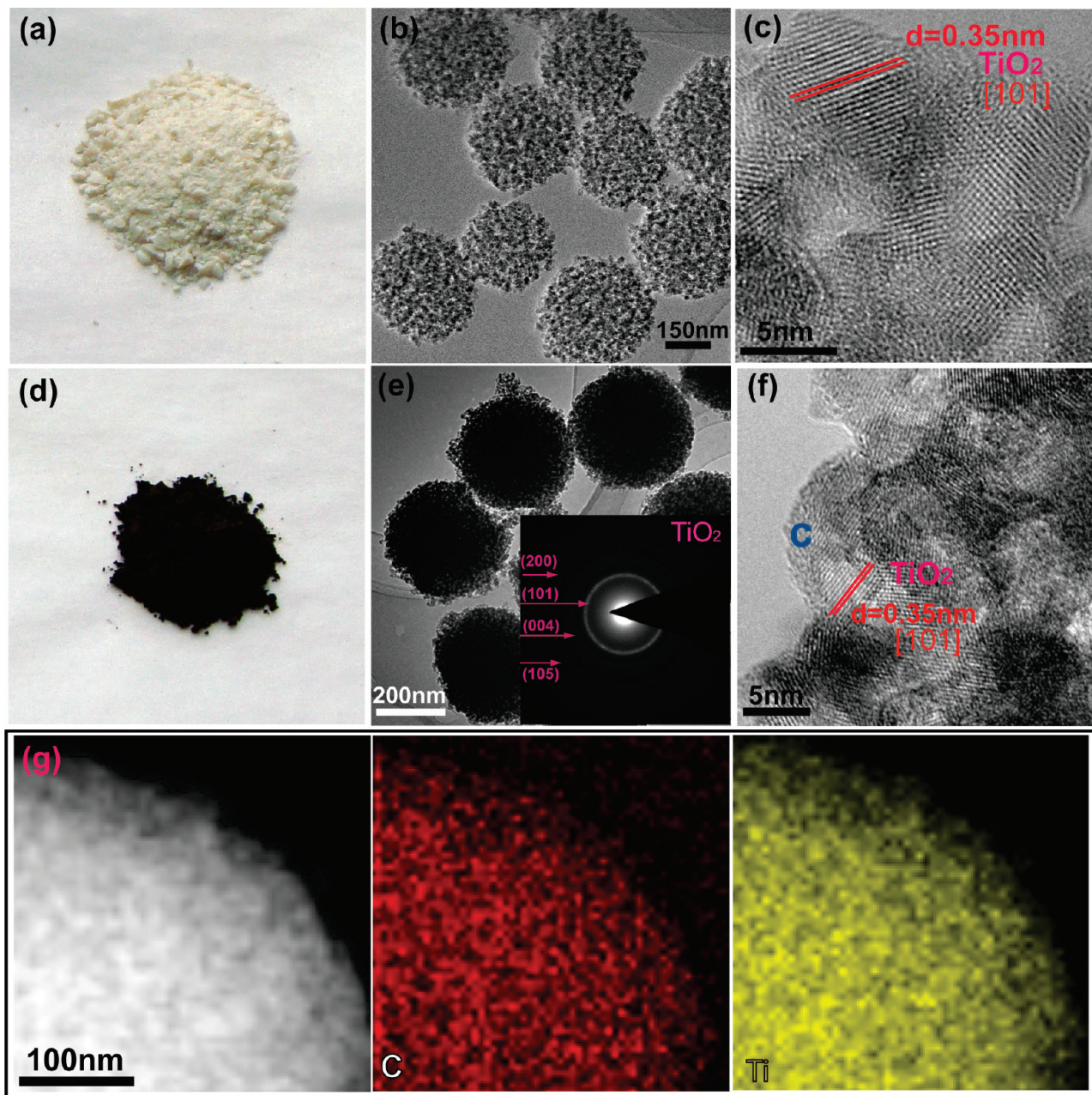


Figure 1. The photograph of pristine porous TiO₂ and TiO₂-C composite: (a) porous TiO₂; (d) TiO₂-C composite. Morphology of TiO₂ and TiO₂-C composite: (b) representative transmission electron microscopy (TEM) image of TiO₂; (c) high-resolution transmission electron microscopy (HRTEM) image of TiO₂; (e) TEM image of TiO₂-C composite; (f) HRTEM image of TiO₂-C composite (the inset shows the SAED pattern of TiO₂-C composite); and (g) elemental mapping of TiO₂-C composite: annual dark-field TEM image of TiO₂-C composite and corresponding C and Ti EDX maps.

2. Experimental Section

2.1. Synthesis of Nanoporous TiO₂. In a typical procedure, 10 mL of tetrabutoxytitanium (Beijing Chemicals Co.) was added to 250 mL of ethylene glycol (Beijing Chemicals Co.) and the solution was magnetically stirred for 8 h at room temperature, then the mixture was poured into a solution containing 850 mL of acetone (Beijing Chemicals Co.) and 13.5 mL of water and vigorous stirred for an hour. The white precipitate was harvested by centrifugation, followed by washing with ethanol for five times. Then it was added to 300 mL of water and refluxed for 1 h. White precipitate was collected by centrifugation followed by washing with water for five times.

2.2. Synthesis of TiO₂-C Nanosphere. A 300 mg porous TiO₂ nanosphere was dispersed in 30 mL of DI water under stirring for 30 min and then 30 mg of glucose (C₆H₁₂O₆·3H₂O)

was added under stirring for 30 min. The resulting suspension was transferred to a 40 mL Teflon autoclave, which was then heated at 180 °C for 12 h. The dark gray product was harvested by centrifugation and washed with DI water, then dried in an oven at 80 °C. The dried precursor was laid in Ar atmosphere annealing at 400 °C for 4 h. The rate of heating is 5 deg/min.

2.3. Structural Characterization. The products were characterized by SEM (JEOL 6701F), energy-dispersive X-ray spectroscopy (EDX, Phoenix), and TEM (Tecnai F20 TEM) with an accelerating voltage of 300 kV. The XRD patterns were obtained by a Rigaku D/max-2500, using filtered Cu K α radiation. The nitrogen adsorption and desorption isotherms at 77.3 K were obtained with a Nova 2000e Surface Area-Pore Size Analyzer. TG was carried out with a Diamond TG-DTA Perkin-Elmer-SII instrument under air from 40 to 900 °C.

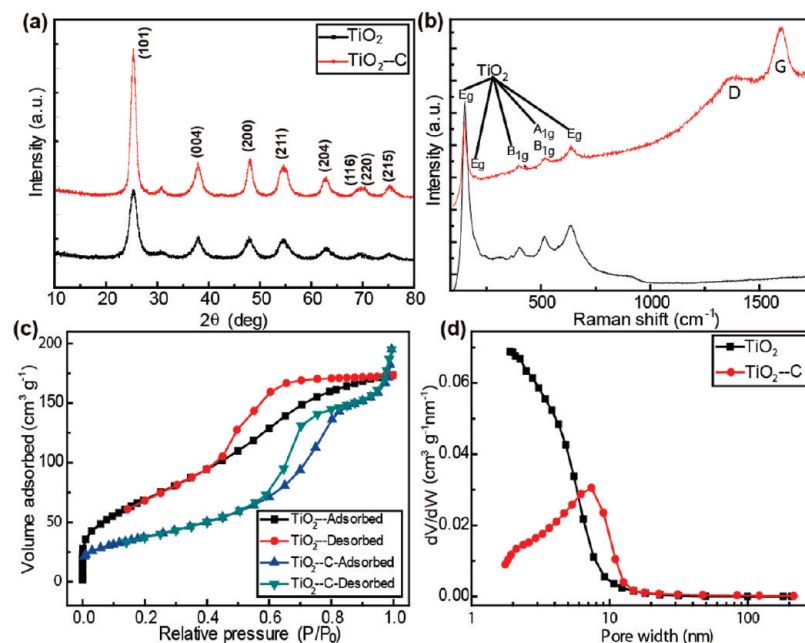


Figure 2. (a) X-ray diffraction patterns: porous TiO_2 , $\text{TiO}_2\text{-C}$ nanosphere (red); (b) Raman spectra of porous TiO_2 , $\text{TiO}_2\text{-C}$ nanosphere (red); (c) nitrogen adsorption/desorption isotherms of $\text{TiO}_2\text{-C}$ nanosphere and TiO_2 ; (d) the pore size distribution plot of $\text{TiO}_2\text{-C}$ nanosphere (red) and TiO_2 , which was calculated by BJH formula in the adsorption branch isotherm.

2.4. Electrochemical Characterization. Electrochemical experiments were performed with Swagelok-type cells assembled in an argon-filled glovebox. For preparing working electrodes, a mixture of active material, super-P acetylene black, and poly(vinyl difluoride) (PVDF) at a weight ratio of 80:10:10 was pasted on a Cu foil. The loading mass of active materials is about 10 mg cm^{-2} . The counter electrode was either lithium foil (half cell) or $\text{LiFePO}_4\text{-C}^{11}$ (full cell). The latter electrode consisted of 80 wt % $\text{LiFePO}_4\text{-C}$, 10 wt % super-P acetylene black, and 10 wt % PVDF per aluminum foil. In the full cell, $\text{TiO}_2\text{-C}$ is slightly excess over $\text{LiFePO}_4\text{-C}$, and the specific capacity is calculated based on the mass of $\text{TiO}_2\text{-C}$. A glass fiber (GF/D) from Whatman was used as a separator. The electrolyte consisted of a solution of 1 M LiPF_6 in ethylene carbonate/dimethyl carbonate/diethyl carbonate (1:1:1, in wt %) obtained from Tianjin Jinniu Power Sources Material Co., Ltd. Galvanostatic cycling tests of the assembled cells were carried out on an Arbin BT2000 system in the voltage range of 1–3 V.

3. Results and Discussion

To investigate the structure evolution of $\text{TiO}_2\text{-C}$ nanospheres well, monodispersed mesoporous TiO_2 nanospheres with an average diameter of ca. 350 nm (Figure 1a–c) were also fabricated for comparison. The as-prepared $\text{TiO}_2\text{-C}$ nanocomposites show a deep-dark powdered appearance (Figure 1d) compared with white TiO_2 nanospheres (Figure 1a), indicating that carbon has been successfully introduced into TiO_2 . The TEM image shown in Figure 1e and the selected-area electron diffraction (SAED) pattern (inset in Figure 1e) matching well with those of typical anatase TiO_2 further confirm that well-ordered and uniform porous $\text{TiO}_2\text{-C}$ nanospheres have been obtained. In addition, the uniform distribution of carbon-coating layers on/in TiO_2 spheres may be demonstrated by the Ti and C maps of $\text{TiO}_2\text{-C}$ nanospheres (Figure 1g). In the HRTEM image (Figure 1f), crystalline planes of TiO_2 (101) with a distance spacing of 0.35 nm can be clearly observed,¹⁶ whereas no significant crystalline plane of carbon is found, suggesting

its amorphous nature. Instead of altering the nanostructure of initial TiO_2 nanospheres, the as-deposited carbon layer forms a 3D interconnected network and helps to stabilize the sphere-like morphology of $\text{TiO}_2\text{-C}$ nanocomposites, as evident in the HRTEM image of the outer edge of a $\text{TiO}_2\text{-C}$ sphere (Figure 1f).

Various characterizations have been performed to further confirm the structure of the $\text{TiO}_2\text{-C}$ nanosphere. The XRD patterns of porous TiO_2 and $\text{TiO}_2\text{-C}$ nanospheres are shown in Figure 2a, in which all intense peaks in the spectra can be well indexed to anatase TiO_2 (JCPDS Card No. 21-1272) except for a small diffraction peak at about 30.8° , corresponding to brookite TiO_2 (JCPDS Card No. 29-1360). No significant peaks of carbon are observed even after the precursor is heat treated under Ar atmosphere, which is consistent with the HRTEM observation (Figure 1f).

Raman spectra are further employed to confirm the crystalline phase of TiO_2 and the existence of carbon in the $\text{TiO}_2\text{-C}$ nanosphere (Figure 2b). The five Raman modes with strong intensities at 145, 196, 395, 515, and 635 cm^{-1} are seen in both of them, which are in good agreement with the typical Raman features of anatase TiO_2 phase and confirm that TiO_2 is of the same anatase phase before and after carbon coating.²³ The two characteristic peaks located at about 1372 and 1592 cm^{-1} in the Raman spectrum of the $\text{TiO}_2\text{-C}$ nanosphere correspond to the D-band and G-band of carbon, respectively. The low peak-integrated intensity of D-band to G-band indicates the existence of disorder carbon structure, which is consistent with the above XRD and HRTEM results.

N_2 adsorption–desorption isotherms were employed to investigate the possible porous structures of the TiO_2 spheres before and after carbon coating (Figure 2c). The isotherms are identified as type IV, which are typical characters of mesoporous materials.^{22,24} The Brunauer–Emmett–Teller (BET) specific surface areas of TiO_2 and $\text{TiO}_2\text{-C}$ nanosphere are 257 and $136 \text{ m}^2 \text{ g}^{-1}$, respectively. The decrease of the BET specific surface area after carbon coating could be attributed to the fill of carbon in the pores, which is further confirmed by the Barrett–Joyner–

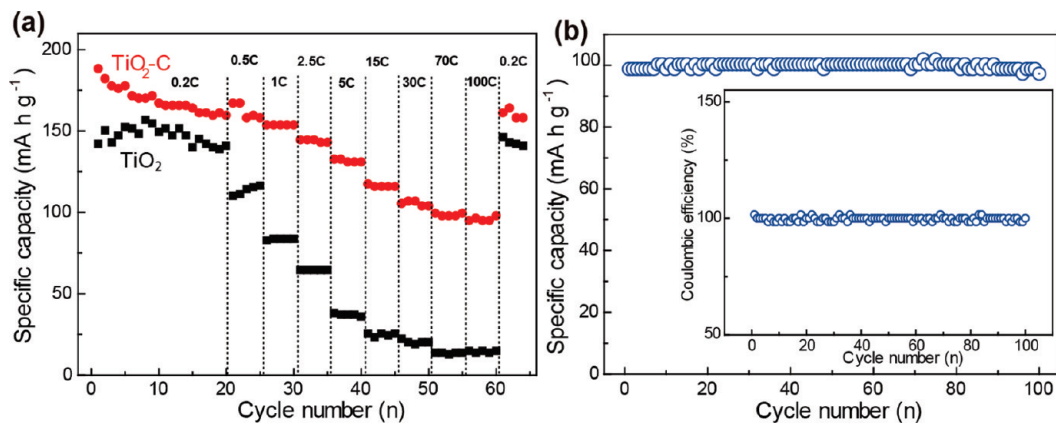


Figure 3. (a) Comparison of the rate capabilities of TiO₂–C nanosphere and porous TiO₂ at different rates between voltage limits of 1 and 3 V. (b) Cycle performance of TiO₂–C nanosphere cycled at 100 C between voltage limits of 1 and 3 V for 100 cycles.

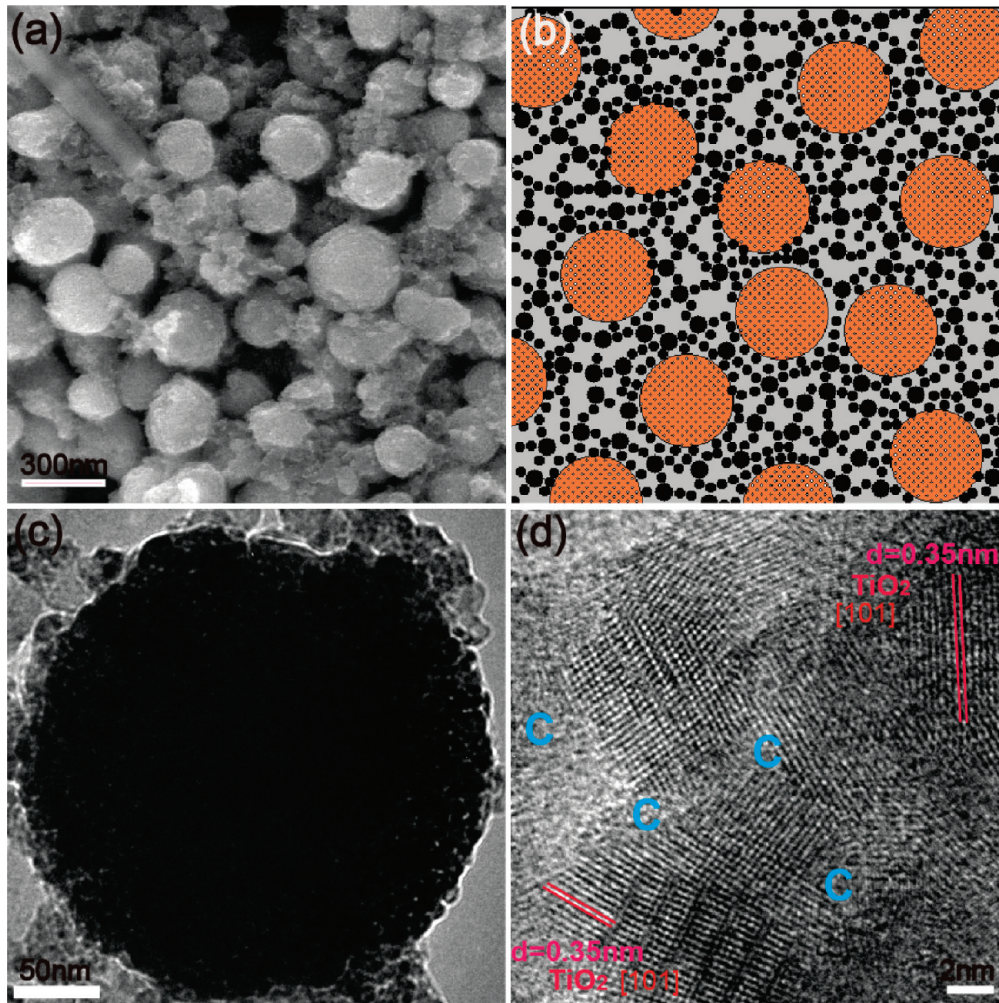


Figure 4. SEM image and TEM images for TiO₂–C nanosphere electrodes after cycling at different rates: (a) SEM image; (b) schematic illustration of the efficient mixed conducting 3D networks formed by the TiO₂–C nanospheres and acetylene black. TiO₂–C (orange); (c) TEM image and (d) HRTEM image.

Halenda (BJH) pore size distribution of TiO₂ and TiO₂–C (Figure 2d). It is found that the pores range from 2 to 10 nm in pristine TiO₂ spheres.²² After carbon coating the sample has a narrower pore-size distribution with an average pore size of about 7 nm. The result indicates that smaller pores disappear and bigger pores become smaller after carbon coating of the mesoporous sphere. Thermogravimetric (TG) analysis was used to determine the chemical composition of the final nanospheres

(see the Supporting Information, Figure S1). The result shows that there is about 6 wt % carbon existing in the TiO₂–C spheres.

Having considered the fabrication of TiO₂–C nanosphere, the next question is about its electrochemical activity, especially rate performance when applied as electrode material. It was found that the TiO₂–C nanosphere exhibits much better rate capability than bare mesoporous TiO₂ when used in half-cells

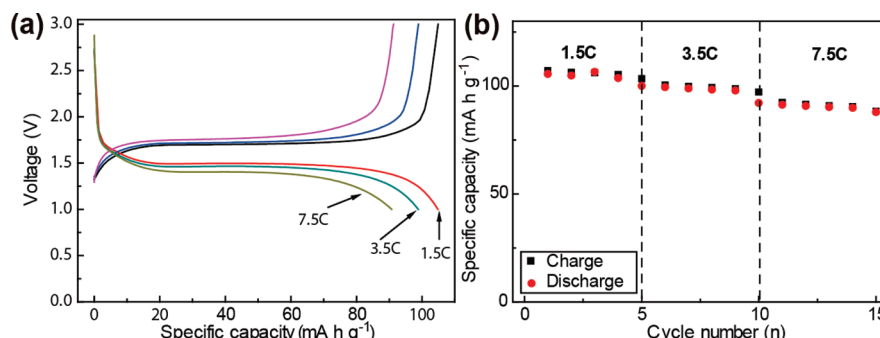


Figure 5. (a) Galvanostatic discharge-charge curves of $\text{TiO}_2\text{-C}/\text{LiFePO}_4\text{-C}$ lithium ion cell between voltage limits of 1 and 3 V. (b) Rate performance of $\text{TiO}_2\text{-C}/\text{LiFePO}_4\text{-C}$ lithium ion cell at different rates between voltage limits of 1 and 3 V.

containing Li foil as the counter electrode (Figure 3a). As the discharge/charge rate increases from 0.2 to 100 C, the specific capacity of the bare TiO_2 sphere drops significantly, while the specific capacity decreases very slowly for $\text{TiO}_2\text{-C}$ nanosphere cycled at the same rates. At the extremely high rate of 100 C (discharge/charge within 36 s), the $\text{TiO}_2\text{-C}$ nanosphere can still have a Li insertion/extraction plateau and deliver a specific capacity as high as 96 mA h g^{-1} , which is much higher than that of the bare mesoporous TiO_2 sphere (near zero). The performance at such a high rate is much better than that of commercial TiO_2 , amorphous TiO_2 ,²⁵ mesoporous anatase TiO_2 ,²⁴ $\text{TiO}_2\text{-B}$ nanowires,²⁶ and nanosized rutile TiO_2 .^{27,28} The only result that may come close to ours has been reported by Jiang et al. on fine anatase powder of 6 nm.²⁹ These authors used a high content of acetylene carbon black (ca. 45 wt %) when testing the anatase, while we only use 10 wt %. When the current density is lowered to 0.2 C again, the specific capacity of 160 mA h g^{-1} could be recovered for $\text{TiO}_2\text{-C}$ nanosphere, demonstrating its good reversibility. In addition to the extremely good rate performance, the $\text{TiO}_2\text{-C}$ nanosphere exhibits also excellent cycle performance. There is nearly no specific capacity loss over 100 cycles at 100 C (Figure 3b). The stable cycling properties imply the chemical/mechanical robustness of the nanosphere, which will be discussed in detail in the following.

The much improved electrochemical performance of the $\text{TiO}_2\text{-C}$ nanosphere could be attributed the efficient mixed conducting 3D networks established when admixed with electronically conducting carbon black additive, as shown in the SEM image of the nanospheres on electrode foils (Figure 4a) and the schematic illustration in Figure 4b. The 3D networks contained two effectively mixed conducting networks, one on the nanoscale and the other on the microscale. Therefore, they could provide shorter lengths for both Li^+ diffusion and e^- transport as well as quick liquid electrolyte penetration, and guarantee the high rate capability.^{16,30,31} Comparing the TEM images of the $\text{TiO}_2\text{-C}$ nanospheres before (Figure 1e,f) and after use (Figure 4c,d) as electrodes in lithium batteries, it is found that the $\text{TiO}_2\text{-C}$ nanosphere can still maintain the nanosphere shape as well as the anatase phase, which is confirmed by the clear (101) planes of anatase with a distance spacing of 0.35 nm in the HRTEM image (Figure 4d). The results indicate that the $\text{TiO}_2\text{-C}$ nanosphere is an electrochemically stable structure toward Li^+ intercalation/extraction.

As mentioned before, the main goal was to obtain new high rate 1.5 V rechargeable Li ion full cells to replace the present 1.5 V alkaline batteries and dry cells. This leads us to the next issue, i.e., the feasibility of $\text{TiO}_2\text{-C}$ nanosphere as a high-rate anode material in a Li ion full battery system with $\text{LiFePO}_4\text{-C}$ as the cathode material.¹¹ The galvanostatic discharge-charge

curves of $\text{TiO}_2\text{-C}/\text{LiFePO}_4\text{-C}$ full cell cycled at different rates between voltage limits of 1 and 3 V are shown Figure 5a. All three discharge curves show a long plateau at about 1.5 V indicating an ideal battery system. The plateau capacity can account for 88% and 86% of its overall capacity at 1.5 and 3.5 C, respectively. At the high rate of 7.5 C, the plateau capacity can still retain 77% of its total capacity. It should be noted that the $\text{TiO}_2\text{-C}/\text{LiFePO}_4\text{-C}$ cell can deliver 88% of its initial capacity (1.5 C) at the higher rate of 7.5 C, demonstrating the excellent high-rate capability of the 1.5 V rechargeable battery. In addition, the full battery exhibits also outstanding charge/discharge efficiency and capacity retention as evident in Figure 5b. The results imply that the full cell is an ideal candidate for replacing nonrechargeable alkaline batteries and dry cells with a nominal voltage of 1.5 V without any change of external circuits of current electronic devices but rechargeable and powerful.

4. Conclusions

In summary, we have developed a simple and cost-effective route for fabricating hierarchically nanostructured TiO_2 electrodes with efficient mixed conducting 3D networks. A key to its realization is, besides the preparation of mesopores, the use of a suitable and cost-saving electronic conductor—here the carbon reduces the diffusion length of lithium ions and enhances electronic conductivity. The as-obtained mesoporous $\text{TiO}_2\text{-C}$ nanosphere can be used as anode material for a new high-rate 1.5 V rechargeable Li ion full cell containing a $\text{LiFePO}_4\text{-C}$ cathode with similar mixed conducting 3D networks. This type of rechargeable battery typically gives an output of 1.5 V per cell, which raises the potential for directly replacing the widely used 1.5 V primary alkaline batteries and dry cells.

Acknowledgment. This work is supported by the National Natural Science Foundation of China (Grant Nos. 20821003, 50730005, and 20701038), National Key Project on Basic Research (Grant Nos. 2006CB806100 and 2009CB930400), and the Knowledge Innovation Program of the Chinese Academy of Sciences (No. KJCX2-YW-W26).

Supporting Information Available: Thermogravimetric curve of $\text{TiO}_2\text{-C}$ nanosphere. This material is available free of charge via the Internet at <http://pubs.acs.org>.

References and Notes

- (1) Kohler, U.; Antonius, C.; Bauerlein, P. *J. Power Sources* **2004**, 127, 45–52.
- (2) Ohms, D.; Kohlhase, M.; Benczur-Urmossy, G.; Schadlich, G. *J. Power Sources* **2002**, 105, 127–133.

- (3) Morioka, Y.; Narukawa, S.; Itou, T. *J. Power Sources* **2001**, *100*, 107–116.
- (4) Feng, F.; Geng, M.; Northwood, D. O. *Int. J. Hydrogen Energy* **2001**, *26*, 725–734.
- (5) Ovshinsky, S. R.; Fetchenko, M. A.; Ross, J. *Science* **1993**, *260*, 176–181.
- (6) Maier, J. *Nat. Mater.* **2005**, *4*, 805–815.
- (7) Bruce, P. G. *Solid State Sci.* **2005**, *7*, 1456–1463.
- (8) Long, J. W.; Dunn, B.; Rolison, D. R.; White, H. S. *Chem. Rev.* **2004**, *104*, 4463–4492.
- (9) Taberna, P. L.; Mitra, S.; Poizot, P.; Simon, P.; Tarascon, J. M. *Nat. Mater.* **2006**, *5*, 567–573.
- (10) Armand, M.; Tarascon, J. M. *Nature* **2008**, *451*, 652–657.
- (11) Wu, X.-L.; Jiang, L.-Y.; Cao, F.-F.; Guo, Y.-G.; Wan, L.-J. *Adv. Mater.* **2009**, *21*, 2710–2714.
- (12) Kang, B.; Ceder, G. *Nature* **2009**, *458*, 190–193.
- (13) Armstrong, G.; Armstrong, A. R.; Bruce, P. G.; Reale, P.; Scrosati, B. *Adv. Mater.* **2006**, *18*, 2597–2600.
- (14) See-How, N.; Nicolas, T.; Bramnik, K. G.; Hartmut, H.; Novák, P. *Chem.—Eur. J.* **2008**, *14*, 11141–11148.
- (15) Huang, S. Y.; Kavan, L.; Exnar, I.; Gratzel, M. *J. Electrochem. Soc.* **1995**, *142*, L142–L144.
- (16) Guo, Y. G.; Hu, Y. S.; Sigle, W.; Maier, J. *Adv. Mater.* **2007**, *19*, 2087–2091.
- (17) Bruce, P. G.; Scrosati, B.; Tarascon, J. M. *Angew. Chem., Int. Ed.* **2008**, *47*, 2930–2946.
- (18) Yang, Z. G.; Choi, D.; Kerisit, S.; Rosso, K. M.; Wang, D. H.; Zhang, J.; Graff, G.; Liu, J. *J. Power Sources* **2009**, *192*, 588–598.
- (19) Poizot, P.; Laruelle, S.; Gruegeon, S.; Dupont, L.; Tarascon, J. M. *Nature* **2000**, *407*, 496–499.
- (20) Morishita, T.; Hirabayashi, T.; Okuni, T.; Ota, N.; Inagaki, M. *J. Power Sources* **2006**, *160*, 638–644.
- (21) Moriguchi, I.; Hidaka, R.; Yamada, H.; Kudo, T.; Murakami, H.; Nakashima, N. *Adv. Mater.* **2006**, *18*, 69–73.
- (22) Zhong, L.-S.; Hu, J.-S.; Wan, L.-J.; Song, W.-G. *Chem. Commun.* **2008**, 1184–1186.
- (23) Miao, Z.; Xu, D.; Ouyang, J.; Guo, G.; Zhao, X.; Tang, Y. *Nano Lett.* **2002**, *2*, 717–720.
- (24) Guo, Y.-G.; Hu, Y.-S.; Maier, J. *Chem. Commun.* **2006**, 2783–2785.
- (25) Hibino, M.; Abe, K.; Mochizuki, M.; Miyayama, M. *J. Power Sources* **2004**, *126*, 139–143.
- (26) Wei, M. D.; Qi, Z. M.; Ichihara, M.; Honma, I.; Zhou, H. S. *Chem. Phys. Lett.* **2006**, *424*, 316–320.
- (27) Jiang, C. H.; Honma, I.; Kudo, T.; Zhou, H. S. *Electrochim. Solid-State Lett.* **2007**, *10*, A127–A129.
- (28) Hu, Y. S.; Kienle, L.; Guo, Y. G.; Maier, J. *Adv. Mater.* **2006**, *18*, 1421–1426.
- (29) Jiang, C. H.; Wei, M. D.; Qi, Z. M.; Kudo, T.; Honma, I.; Zhou, H. S. *J. Power Sources* **2007**, *166*, 239–243.
- (30) Cao, F.-F.; Guo, Y.-G.; Zheng, S.-F.; Wu, X.-L.; Jiang, L.-Y.; Bi, R.-R.; Wan, L.-J.; Maier, J. *Chem. Mater.* **2010**, *22*, 1908–1914.
- (31) Guo, Y.-G.; Hu, J.-S.; Wan, L.-J. *Adv. Mater.* **2008**, *20*, 2878–2887.

JP103218U

Supporting Information for

Facile Synthesis of Mesoporous TiO₂-C Nanosphere as an Improved Anode Material for Superior High Rate 1.5V Rechargeable Li-Ion Batteries Containing LiFePO₄-C Cathode

*Fei-Fei Cao,[†] Xing-Long Wu,[†] Sen Xin,[†] Yu-Guo Guo** and *Li-Jun Wan**

Beijing National Laboratory for Molecular Sciences, Institute of Chemistry, Chinese Academy of Sciences (CAS), Beijing 100190 (P. R. China)

[†] Also at the Graduate School of CAS, Beijing 100064, China

* To whom correspondence should be addressed. E-mail: yguo@iccas.ac.cn
(Y.-G.G.), wanlijun@iccas.ac.cn (L.-J.W.).

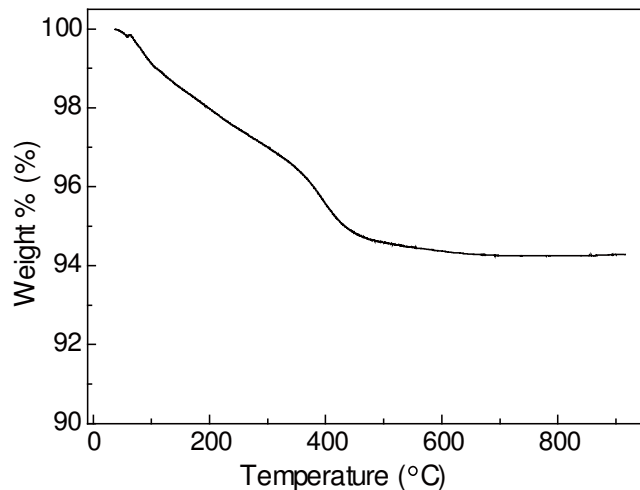


Figure S1. Thermogravimetric curves of TiO₂-C nanosphere. This experiment was carried out under air atmosphere at temperature range from 30 °C to 900 °C.